

# Wave kinetics of drift-wave turbulence and zonal flows beyond the ray approximation

Hongxuan Zhu,<sup>1,2</sup> Yao Zhou,<sup>2</sup> D. E. Ruiz,<sup>3</sup> and I. Y. Dodin<sup>1,2</sup>

<sup>1</sup>*Department of Astrophysical Sciences, Princeton University, Princeton, NJ, 08544*

<sup>2</sup>*Princeton Plasma Physics Laboratory, Princeton, NJ 08543*

<sup>3</sup>*Sandia National Laboratories, P.O. Box 5800, Albuquerque, New Mexico 87185, USA*

Inhomogeneous drift-wave turbulence can be modeled as an effective plasma where drift waves act as quantumlike particles and the zonal-flow velocity serves as a collective field through which they interact. We report the first Wigner–Moyal simulations of this effective plasma (within the generalized Hasegawa–Mima model assumed for simplicity), i.e., kinetic simulations of the ray phase-space dynamics with full-wave effects retained. We also demonstrate how the quantumlike approach facilitates calculations and analysis of the zonal-flow formation and deterioration, including the predator-prey oscillations and the emergence of the Rayleigh–Kuo criterion. In contrast, the traditional wave kinetic equation misses essential physics and is insufficient for modeling of these effects.

*Introduction.* – Interactions between zonal flows (ZFs) and drift-wave (DW) turbulence are a fundamental problem in plasma physics and fusion science and has been actively studied for many years [1]. One of the common models for studying these interactions is the wave kinetic equation (WKE) [2–11], which relies on the geometrical-optics (GO) approximation; i.e., the DW wavelengths are assumed negligible compared to those of ZFs. However, this assumption is not always justified [12–15], and essential physics is lost in the GO limit [16, 17]. (Additional evidence of that is also presented below.) This stimulated formulations of “full-wave” statistical theories, which can still be manageable if the quasilinear approximation is invoked, i.e., the eddy-eddy interactions are ignored. A particularly notable example is the second-order cumulant expansion (CE2), which has been enjoying applications both in geophysics and plasma physics [18–21]. However, since the CE2 is formulated in terms of a two-point spatial correlation function, it is not clear how it is an obvious generalization of the WKE, which describes the DW dynamics in the ray phase space. Thus, an alternative theory is needed to unify the WKE and the full-wave approach to inhomogeneous turbulence.

More recently, it was noticed [17] that the DW dynamics in a prescribed ZF can be viewed as the dynamics of scalar quantum particles with a non-Hermitian Hamiltonian. Also, the evolution of the ZF velocity can be expressed in terms of the DW Wigner function, which can be considered as a quasiprobability distribution of DW quanta (“driftons”) in phase space. Hence, a full-wave kinetic model of inhomogeneous DW turbulence can be formulated like the kinetic equation of a quantumlike plasma, i.e., the Wigner–Moyal (WM) equation [22, 23]. This approach is based on the same assumptions as the CE2 but describes the DW dynamics in terms of phase-space variables. Hence, it benefits from the existing machinery of quantum kinetics and Hamiltonian mechanics, and it also provides a direct link with the WKE, which is subsumed by the WM equation as the GO limit. It was also found that this limit is not *quite* the traditional WKE (tWKE) but includes corrections

that reinstate the conservation of the DW–ZF total enstrophy as opposed to the DW enstrophy. Applications of this “improved” WKE (iWKE) [24] were recently contemplated in Refs. [16, 17], but the utility of full-wave WM modeling of DW turbulence has not been explored until now.

Here, we report the first WM simulations of DW turbulence using the mathematical formalism developed in Ref. [17]. These simulations can be understood as the first numerical modeling of DW turbulence as kinetics of an effective plasma where DWs act as quantumlike particles and the ZF velocity serves as a collective field. We also demonstrate how the WM approach facilitates calculations and analysis of the ZF formation and deterioration and reveals the importance of full-wave effects missing in the tWKE and iWKE. For the linear zonostrophic instability (ZI) [4, 5, 18–20], when the tWKE dynamics is simulation-box dependent and the iWKE is only qualitatively accurate, the WM model predicts physical rates that account for full-wave effects and agree with the CE2. We also show, both analytically and numerically, that the DW–ZF predator–prey-type oscillations [2, 6, 10] occur outside the validity domain of their existing theory but are readily seen in WM simulations *ab initio*. In this sense, our WM model is the first accurate DW-kinetic model of these oscillations. Likewise, the tertiary instability (TI) of strong ZFs [7, 15, 25–28] cannot be described by the tWKE or the iWKE but is captured by the WM analysis. We calculate the TI growth rate and mode structure and compare our results with simulations. Also, we show that the famous Rayleigh–Kuo (RK) criterion of the ZF stability [29], which so far had no place in DW kinetics, is naturally subsumed under the WM formulation. Importantly, the specific turbulence model assumed below is just an example chosen for its simplicity and relevance to the well-known tWKE and CE2 simultaneously. Perhaps this can help bridge the communities using those formulations. More complex turbulence models also can be represented in the WM form but those are not discussed here.

*Basic equations.* – Our plasma model is as follows.

We assume cold ions, electrons with temperature  $T_e$ , and a uniform magnetic field  $\mathbf{B}_0 = B_0 \hat{\mathbf{z}}$ , where  $\hat{\mathbf{z}}$  is a unit vector along the  $z$  axis. The equilibrium density gradient  $\nabla n_0$  is assumed in the  $y$  direction. Then, the electrostatic potential  $\varphi$  can be described by the generalized Hasegawa–Mima equation (gHME) [4, 5, 30, 31]

$$\partial_t w + (\hat{\mathbf{z}} \times \nabla \varphi) \cdot \nabla w + \beta \partial_x \varphi = 0, \quad w = (\nabla^2 - \hat{a}) \varphi$$

for the generalized vorticity  $w(t, \mathbf{x})$  on the  $\mathbf{x} \equiv (x, y)$  plane transverse to  $\mathbf{B}_0$ . Here, time is measured in units  $\Omega_i^{-1}$ , where  $\Omega_i$  is the ion gyrofrequency; length is measured in units of the plasma sound radius  $\rho_s \doteq c_s/\Omega_i$  (the symbol  $\doteq$  denotes a definition), where  $c_s$  is the ion sound speed;  $\varphi$  is measured in units  $T_e/|e|$ , where  $e$  is the electron charge; also,  $\beta$  is proportional to  $\partial_y n_0$  and is treated as a positive constant. The operator  $\hat{a}$  models the electron response to  $\varphi$  such that  $\hat{a} = 1$  for DWs and  $\hat{a} = 0$  for ZFs [31]. External forcing and dissipation are not included because they are not directly relevant to the effects discussed below. If the stochastic forcing were retained, ergodicity in the  $x$  direction would have to be assumed, like in the CE2 [20].) For any given field  $f$ , we introduce its zonal average as  $\langle f \rangle \doteq \int f dx / L_x$  (here,  $L_x$  is the system length in the  $x$  direction) and fluctuations as  $\tilde{f} \doteq f - \langle f \rangle$ . ZFs are described by the zonal-averaged velocity  $U(t, y) \doteq -\langle \varphi' \rangle$ . (The prime denotes the derivative with respect to  $y$ .) Assuming the quasi-linear approximation, DWs are governed by an equation of the Schrödinger form,  $i \partial_t \tilde{w} = \hat{H} \tilde{w}$ , where  $\hat{H}$  is understood as the driftion Hamiltonian [17]. We also introduce the zonal-averaged Wigner function  $W(t, y, \mathbf{p}) \doteq \langle \int e^{-i\mathbf{p} \cdot \mathbf{s}} \tilde{w}(t, \mathbf{x} + \mathbf{s}/2) \tilde{w}(t, \mathbf{x} - \mathbf{s}/2) d^2 s \rangle$ . Then, the WM formulation is given by [17]

$$\partial_t W = \{\{\mathcal{H}, W\}\} + [[\Gamma, W]], \quad (1)$$

$$\partial_t U = \partial_y \int p_D^{-2} \star p_x p_y W \star p_D^{-2} d^2 p / (2\pi)^2. \quad (2)$$

Here,  $\mathcal{H}$  and  $\Gamma$  are the Weyl symbols of the Hermitian and anti-Hermitian parts of  $\hat{H}$ , specifically,

$$\mathcal{H} = -\frac{\beta p_x}{p_D^2} + p_x U + \frac{1}{2} [[U'', \frac{p_x}{p_D^2}]], \quad \Gamma = \frac{1}{2} \{\{U'', \frac{p_x}{p_D^2}\}\},$$

and  $p_D^2 \doteq 1 + p_x^2 + p_y^2$ . Also,  $\star$  is the Moyal star,  $A \star B \doteq A e^{i\hat{\mathcal{L}}/2} B$ , where  $\hat{\mathcal{L}} \doteq \hat{\partial}_{\mathbf{x}} \cdot \hat{\partial}_{\mathbf{p}} - \hat{\partial}_{\mathbf{p}} \cdot \hat{\partial}_{\mathbf{x}}$  and the arrows indicate the directions in which the derivatives act. For example,  $A \hat{\mathcal{L}} B$  is the canonical Poisson bracket,  $\{A, B\}$ . Also,  $\{\{A, B\}\} \doteq 2A \sin(\hat{\mathcal{L}}/2) B$  and  $[[A, B]] \doteq 2A \cos(\hat{\mathcal{L}}/2) B$  are the (Moyal) sine and cosine brackets. We solve these equations numerically using the spectral representation proposed in Ref. [17]. The accuracy of this model is the same as of the CE2 [18–21]. Similar equations can also be formulated for turbulence models other than the gHME, so the latter is only an example. (For multi-component wave systems,  $\mathcal{H}$ ,  $\Gamma$ , and  $W$  are generally tensors.)

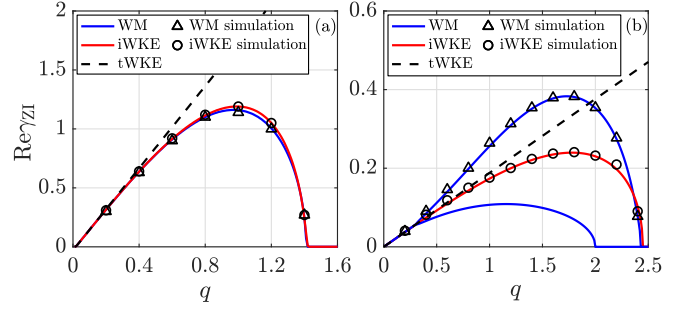


FIG. 1. The ZI growth rate  $\gamma_{\text{ZI}}(q)$  for two equilibrium distributions: (a)  $\mathcal{W}_1$  with  $\mathcal{N} = 50$  and  $p_f = 1$  (because DW turbulence is expected at scales  $\sim \rho_s$  [12]); (b)  $\mathcal{W}_2$  with  $k_x = 2$ ,  $k_y = 1$ , and  $\mathcal{N} = 100/(2\pi)^2$ . In both cases,  $\beta = 1$ . Shown are the analytical results obtained from the WM (blue), iWKE (red), and tWKE (dashed) models, and the corresponding numerical results obtained from the WM (triangles) and iWKE (circles) simulations. The two blue lines in figure (b) correspond to two different branches of  $\text{Re } \gamma_{\text{TI}}$ . Only the fastest-growing mode is observed in simulations.

For comparison, we also introduce the GO limit, which corresponds to  $\max(\lambda_{\text{DW}}/\lambda_{\text{ZF}}, \rho_s/\lambda_{\text{ZF}}) \ll 1$ . (Here,  $\lambda_{\text{DW}}$  is the characteristic DW wavelength and  $\lambda_{\text{ZF}}$  is the ZF spatial scale.) In this limit, Eqs. (1) and (2) become

$$\partial_t W = \{\mathcal{H}, W\} + 2\Gamma W, \quad (3)$$

$$\partial_t U = \partial_y \int p_x p_y p_D^{-4} W d^2 p / (2\pi)^2, \quad (4)$$

which is what we call the iWKE model. Here,  $W$  can be understood as the phase-space probability distribution of driftions,  $\mathcal{H}$  serves as their GO Hamiltonian, and  $\Gamma$  serves as their GO damping rate. Specifically,

$$\mathcal{H} = p_x U + p_x (U'' - \beta)/p_D^2, \quad \Gamma = -U''' p_x p_y / p_D^4. \quad (5)$$

The tWKE has the same general form, Eq. (3), but with  $\mathcal{H} = p_x U - \beta p_x / p_D^2$  and  $\Gamma = 0$  [2–11]. We solve these equations numerically using discontinuous Galerkin methods implemented in the GKEYLL code [17, 32].

*Linear ZI.* – As the first application, we study the linear ZI, which is the formation of ZFs out of homogeneous DW turbulence with some equilibrium Wigner function  $\mathcal{W}(\mathbf{p})$ . Within the WM approach, the ZI growth rate is found just like the kinetic dispersion relation of linear waves in a quantum plasma, except the particle (drifton) Hamiltonian is somewhat unusual. Suppose a ZF velocity  $U = \text{Re}(U_q e^{iqy + \gamma_{\text{ZI}} t})$  and  $\delta W = \text{Re}(W_q e^{iqy + \gamma_{\text{ZI}} t})$ . Then,  $\gamma_{\text{ZI}}$  is expected to satisfy the dispersion relation [17]

$$\gamma_{\text{ZI}} = \int \frac{d^2 p}{(2\pi)^2} \frac{q p_x^2 p_y}{\gamma_{\text{ZI}} p_{D,+q}^2 p_{D,-q}^2 + 2i\beta q p_x p_y} \times \left[ \left(1 - \frac{q^2}{p_{D,-q}^2}\right) \mathcal{W}_{-q} - \left(1 - \frac{q^2}{p_{D,+q}^2}\right) \mathcal{W}_{+q} \right], \quad (6)$$

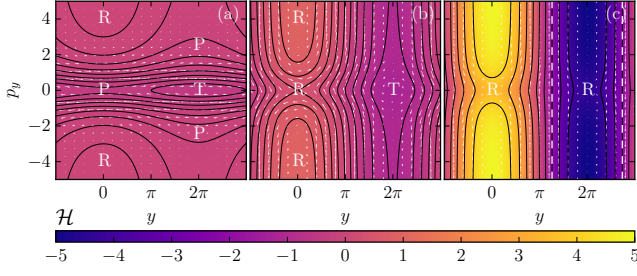


FIG. 2. Contour plots of  $\mathcal{H}$  from the iWKE for  $U = u_0 \cos qy$  at  $\beta = 1$ ,  $q = 0.5$ , and  $p_x = 0.5$ : (a) Regime 1,  $u_0 = 0.1$ ; (b) Regime 2,  $u_0 = 2$ ; and (c) Regime 3,  $u_0 = 10$ . The arrows show the phase-space velocity given by Eqs. (7) and (8). The labels P, T, and R denote passing, trapped, and runaway trajectories, correspondingly. The vertical dashed lines in figure (c) denote the locations where  $U'' = \beta$ .

where  $\mathcal{W}_{\pm q} \doteq \mathcal{W}(p_x, p_y \pm q/2)$  and  $p_{D,\pm q}^2 \doteq 1 + p_x^2 + (p_y \pm q/2)^2$ . For comparison, the iWKE predicts [16]

$$1 = \int \frac{d^2 p}{(2\pi)^2} \frac{q^2 p_x^2 p_D^4 (1 - 4p_y^2/p_D^2)(1 - q^2/p_D^2)}{(\gamma_{\text{ZI}} p_D^4 + 2i\beta q p_x p_y)^2} \mathcal{W}(\mathbf{p}).$$

The tWKE result is obtained if we ignore the term  $q^2/p_D^2$  in the second bracket in the numerator.

We considered two equilibrium distributions:  $\mathcal{W}_1(\mathbf{p}) = 2\pi\mathcal{N}\delta(|\mathbf{p}| - p_f)/p_f$  and  $\mathcal{W}_2(\mathbf{p}) = \pi^2\mathcal{N}\sum_{m_x, y=\pm 1}\delta(p_x - m_x k_x)\delta(p_y - m_y k_y)$ . Here,  $\mathcal{N}[\mathcal{W}] = \int \mathcal{W}(\mathbf{p}) d^2 p / (2\pi)^2$  is the density of driftons, or twice the DW enstrophy density [17], and  $p_f$ ,  $k_x$ , and  $k_y$  are constants. The simulations were performed with  $U(t=0, y) = U_q \cos qy$  (with small  $U_q$ ) and  $W(t=0, y, \mathbf{p}) = \mathcal{W}_{1,2}(\mathbf{p})$ . The exponential growth rates of the perturbations in WM simulations agree with those predicted by Eq. (6) (Fig. 1). In contrast, the tWKE results are adequate only at  $q \ll 1$ , and the corresponding  $\gamma_{\text{ZI}}$  has a maximum at the largest  $q$  resolved in simulations. Thus, the tWKE is inapplicable to modeling the ZI, as also noticed in Refs. [16, 17]. (This means that the pioneering tWKE-based simulations of the ZI in Ref. [9] were only a qualitative demonstration of the effect.) The iWKE is better for it predicts that the ZI vanishes at  $q \gtrsim 1$  and approximates  $\text{Re } \gamma_{\text{ZI}}$  reasonably well in the most important region, namely, at  $q \leq 1$ , where  $\gamma_{\text{ZI}}$  has its maximum. But even so, in general, the iWKE agreement with the full-wave theory is only qualitative [Fig. 1(b)], and the WM model is more adequate.

*Nonlinear ZI.* – Let us also compare the GO and full-wave DW–ZF dynamics beyond the linear ZI. The former can be elucidated by using ray equations inferred from

the iWKE. From Eqs. (3) and (5), one gets

$$\frac{dy}{dt} = \frac{\partial \mathcal{H}}{\partial p_y} = \frac{2p_x p_y}{p_D^4} (\beta + q^2 u_0 \cos qy), \quad (7)$$

$$\frac{dp_y}{dt} = -\frac{\partial \mathcal{H}}{\partial y} = \left(1 - \frac{q^2}{p_D^2}\right) p_x q u_0 \sin qy, \quad (8)$$

where we substituted a fixed ZF profile  $U = u_0 \cos qy$  for clarity. Three different topologies of the phase space  $(y, p_y)$  are possible then, assuming  $q < 1$  [33]. (At  $q > 1$ , additional equilibria appear but the GO model is inapplicable, so it is not considered.) Regime 1 corresponds to weak ZFs, namely,  $u_0 < u_{c,1} \doteq \beta/(2 - q^2)$  (Fig. 2). In this case, there exist three types of trajectories: passing (labeled “P”), trapped (labeled “T”), and runaway (labeled “R”), which extend to infinity in the  $p_y$  space while being localized in the  $y$  space [34]. Regime 2 corresponds to moderate ZFs,  $u_{c,1} \leq u_0 \leq u_{c,2} \doteq \beta/q^2$ . In this case, P-trajectories vanish but T- and R-trajectories persist. Regime 3 corresponds to the situation when only R-trajectories are left. This is the case of strong ZFs,  $u_0 > u_{c,2}$ . The latter is precisely the RK criterion [29], which has been known as a necessary condition of the ZF instability. Note that the RK parameter  $\varrho \doteq u_0/u_{c,2}$  emerges in the iWKE but not in the tWKE, where  $u_{c,2}$  is infinite and hence Regime 3 is impossible.

Since the total energy is conserved [17], the ZI eventually saturates. By taking moments of the iWKE, one also finds that  $\partial_t U = [2(U'' - \beta)]^{-1} \partial_t \mathcal{N}$ . Since the direction of phase-space flows is known (Fig. 2), one can show from here [33] that, within the iWKE validity do-

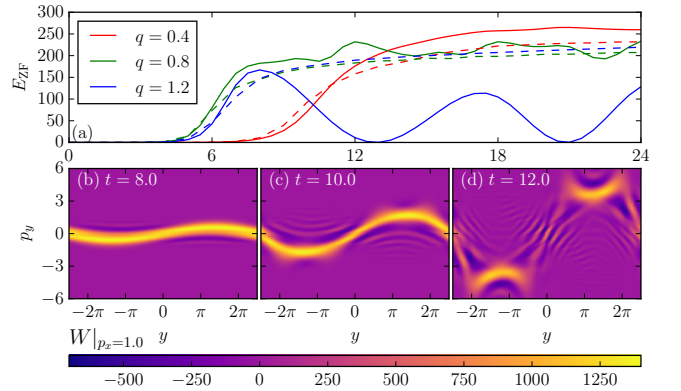


FIG. 3. Nonlinear simulations of the ZI with the same initialization as in Fig. 1(a). (a) The ZF energy  $E_{\text{ZF}} \doteq \int U^2 dy/2$  versus  $t$  for various  $q$ : iWKE model (dashed) and WM model (solid). At  $q \lesssim 1$ , the iWKE and WM models produce similar results. At  $q \gtrsim 1$ , the iWKE (and the tWKE) is inapplicable, while WM simulations predict oscillations of  $E_{\text{ZF}}$ . (b)–(d) Snapshots of  $W$  from WM simulations ( $q = 0.4$ ) for different  $t$ . The centers of the  $\cap$  and  $\cup$ -shaped structures in figure (d) correspond to  $U'' = \beta$ . The shape of these structures is determined by R-trajectories [cf. Fig. 2(c)]. Also see the related movies in the supplementary material [35].

main ( $q < 1$ ), the profile of  $U$  can *only sharpen* with time. This implies that the ZI saturates monotonically, i.e., never transfers its energy back to DWs. This is corroborated by both iWKE and WM simulations at  $q \lesssim 1$ ; i.e., the GO approximation is adequate [Fig. 3(a)]. In contrast, at  $q \gtrsim 1$ , full-wave effects are essential. In this domain, the iWKE (and the tWKE) is inapplicable, while WM simulations show that the ZI is eventually *reversed*; i.e., an intense ZF starts transferring its energy back to DWs (Fig. 3). This results in predator-prey-type oscillations. Such oscillations were also reported in the past [2, 6, 10], but were assumed to require collisional damping of ZFs, which as seen from our simulations is not necessary. Besides, predator-prey oscillations were previously shown only within a tWKE-based model of drifton quasilinear diffusion, which assumes the GO limit and random small-amplitude ZFs. Neither of these assumptions actually holds in the regime when the oscillations occur in our simulations. In this sense, our WM model is the first accurate DW-kinetic model of these oscillations. Also, the importance of  $q$  as a bifurcation parameter is consistent with our TI theory presented below.

*Tertiary instability.* – Suppose an intense ZF set up initially without DWs. Such ZF is subject to an instability of the Kelvin-Helmholtz-type that we term TI. (The presence of DWs in the initial state can affect the instability rate, as shown in Refs. [19, 21] and in the above discussion of the nonlinear ZI. We do not consider this effect here for it is hard to separate such TI from the nonlinear ZI.) This definition of the TI is different from that in Refs. [27, 28], where the TI was attributed to the ion-temperature gradient (absent in our model), but similar to those in the vast majority of the relevant papers [7, 15, 25, 26]. In Refs. [16, 25], a connection was mentioned between the TI and the RK criterion, but the sufficient and necessary conditions for the TI were not explored analytically, and the mode structure remained unknown [36]. Here, we propose two analytical and numerical calculations of the TI, which are as follows [33].

Let us consider  $\tilde{\phi} = \text{Re}[\phi(y)e^{ik_x x - i\omega t}]$  and denote  $C \doteq \omega/k_x$ . Linearizing the gHME for the fluctuations gives

$$\left[ \frac{d^2}{dy^2} - (1 + k_x^2) - \frac{U'' - \beta}{U - C} \right] \phi = 0. \quad (9)$$

For simplicity, we assume  $U = u_0 \cos qy$  and search for  $\phi$  as a Floquet mode,  $\phi = \psi(y)e^{i\bar{q}y}$ , where  $\psi(y + 2\pi/q) = \psi(y)$  and  $\bar{q}$  is a constant restricted to the first Brillouin zone,  $-q/2 \leq \bar{q} < q/2$ . Then, by following and correcting [33] Kuo's original argument [29], we find that there are at most two unstable modes in this case. The maximum of their growth rate, which we denote as the TI growth rate  $\gamma_{\text{TI},1} = \max(k_x \text{Im}C)$ , is given by

$$\gamma_{\text{TI},1} = |k_x u_0| \vartheta H(\vartheta) \sqrt{1 - \varrho^{-2}}, \quad (10)$$

where  $\vartheta \doteq 1 - (\bar{q}^2 + 1 + k_x^2)/q^2$ ,  $\varrho = u_0 q^2/\beta$ , and  $H$  is the Heaviside step function. (The index 1 in  $\gamma_{\text{TI},1}$

denotes that this is our first analytical model of  $\gamma_{\text{TI}}$ .) This growth rate is largest at  $\bar{q} = 0$  and remains positive if  $\varrho > 1$  and  $q^2 > 1 + k_x^2 > 1$ . Similar inequalities hold for nonsinusoidal ZF, as confirmed numerically [33]. Hence, we find that the necessary and sufficient conditions for the TI onset is twofold: (i)  $\varrho \gtrsim 1$  and (ii)  $q^2 \gtrsim 1$  (or, in dimensional variables,  $q^2 \gtrsim \rho_s^{-2}$ ). Note that  $q^2 \gtrsim 1$  implies a violation of the GO approximation. As a corollary, there is no TI in the GO limit. Also note that these findings differ from those in Ref. [7], where the  $\varrho$ -dependence is missed.

For comparison, we also calculated  $\gamma_{\text{TI}}$  numerically as follows. First, we represent Eq. (9) as an eigenvalue problem,  $\hat{A}^{-1}(U\hat{A} + \beta - U'')\psi = C\psi$ , where  $\hat{A} \doteq d^2/dy^2 + 2i\bar{q}d/dy - (\bar{q}^2 + 1 + k_x^2)$ . Then, we search for  $\psi$  in the form  $\psi = \sum_{m=-N}^N \psi_m e^{imqy}$ , where the series is truncated at a large enough  $N$ . Then,  $C$  can be found as an eigenvalue of a  $(2N+1) \times (2N+1)$  matrix. As seen from Fig. 4, Eq. (10) is in reasonable agreement with the simulations but only when  $\vartheta \ll 1$ . In contrast, the WM approach allows for a calculation that extends to general  $\vartheta$ , namely, as follows. The numerical solution of the above eigenmode equation for  $\psi$  can be used to calculate the eigenvector  $\psi_m$ , so we also obtain  $\tilde{w} = (\nabla^2 - 1)\tilde{\varphi}$  and  $W$ . In the spectral representation  $\mathfrak{W}(t, \lambda, \mathbf{p}) \doteq \int W(t, y, \mathbf{p}) e^{-i\lambda y} dy$ , the Floquet mode is a series of delta functions,  $\mathfrak{W}(t, \lambda, \mathbf{p}) = \sum_{mn} \mathfrak{W}_{m,n}(p_x) \delta(\lambda - mq) \delta(p - nq/2)$ , where  $\mathfrak{W}_{m,n}$  decrease with  $m$  and  $n$ . As an approximation, one can retain just few terms, say,  $\mathfrak{W}_{0,0}$ ,  $\mathfrak{W}_{\pm 1, \pm 1}$ ,  $\mathfrak{W}_{\pm 2, 0}$ , and  $\mathfrak{W}_{0, \pm 1}$ . Then, from Eq. (1), we obtain the following eigenvalue

$$\gamma_{\text{TI},2} = |k_x u_0| [\sqrt{2}(1 + \delta)]^{-1} \sqrt{1 - \delta^2 - (2\delta^2 \varrho^2)^{-1}}, \quad (11)$$

where  $\delta \doteq (1 + k_x^2)/q^2$ . The conditions for the TI onset within this model are  $2\varrho^2 \delta^2 (1 - \delta^2) > 1$  and  $\delta^2 < 1$ , i.e.,  $q^2 > 1 + k_x^2$ . This implies  $\varrho > \sqrt{2}$  and  $q^2 > 1$ , which is in qualitative agreement with Eq. (10). Some discrep-

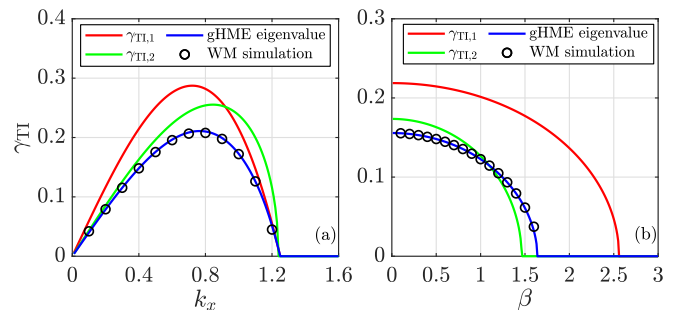


FIG. 4. (a)  $\gamma_{\text{TI}}(k_x)$  at  $\beta = 0.5$  and (b)  $\gamma_{\text{TI}}(\beta)$  at  $k_x = 0.4$ . In both cases,  $U(t = 0, y) = u_0 \cos qy$ ,  $u_0 = 1$ ,  $q = 1.6$ , and  $\bar{q} = 0$ . Shown are the analytical approximations (10) (red) and (11) (green). Also shown are numerical solutions of the eigenvalue equation for  $C$  (blue) and results of WM simulations (circles) with  $W(t = 0, y, \mathbf{p}) \propto \delta(p_x - k_x) e^{-p_y^2}$ .



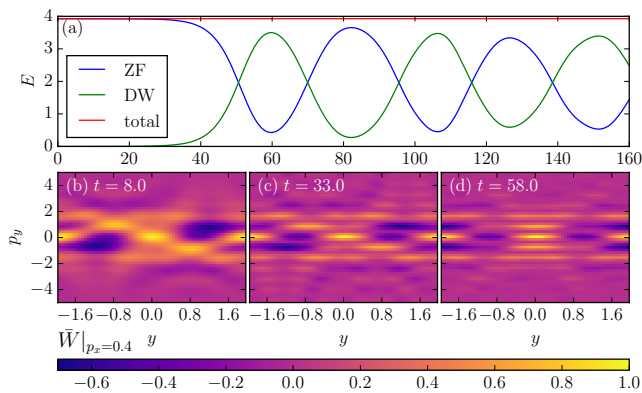


FIG. 5. Nonlinear simulations of the TI with the same initial-ization as in Fig. 4 ( $\beta = 1$ ,  $k_x = 0.4$ ). (a) The energy of the ZF (blue), DWs (green) [17], and the total energy (red) versus  $t$ . (b)-(d) Snapshots of the normalized (to its maximum value at the corresponding  $t$ ) Wigner function  $\bar{W}$  for different  $t$ . Unlike in GO predictions for the saturated TI mode [33], figures (c) and (d) show the presence of multiple harmonics in the  $p_y$  spectrum, which is because DWs are Floquet modes rather than point particles. Also, substantial regions of negative  $\bar{W}$  are present, which is inconsistent with the GO interpretation of  $W$  as a probability distributions. This shows the importance of full-wave effects. The energy oscillations seen in figure (a) are correlated with the horizontal shifts of the phase space structures; compare figures (c) and (d). Also see the related movie in the supplementary material [35].

ancy is explained by the fact that our series truncation is not a rigorous asymptotic approximation. For the same reason,  $\gamma_{\text{TI},2}$  is not *always* a better approximation of  $\gamma_{\text{TI}}$  compared to  $\gamma_{\text{TI},1}$ , but at least it does not require the smallness of  $\vartheta$ . Results of WM simulations of the TI are presented in Fig. 5, which also illustrates the phase-space dynamics during the nonlinear stage. We also note that our findings are in agreement with the direct numerical simulations reported in Ref. [25].

**Conclusions.** – We report the first application of the WM formulation to analytical and numerical modeling of inhomogeneous DW turbulence. In a nutshell, the turbulence is modeled as kinetics of an effective plasma where DWs act as quantumlike particles and the ZF velocity serves as a collective field through which they interact. Our findings show that this formulation provides an efficient and intuitive tool for both analytical and numerical studies of DW kinetics and also reveals the importance of full-wave effects missing in traditional wave kinetics. Although we mainly focus on the ZI and TI within the gHME model, the findings reported here are only examples. Broader applications of the WM formulation to wave turbulence are anticipated in the future.

The authors thank J. B. Parker and J. A. Krommes for valuable discussions, E. L. Shi for sharing GKEYLL and an input script, and C. F. Dong for assistance in using them. The work was supported by the U.S. DOE

through Contract DE-AC02-09CH11466 and by Sandia National Laboratories. Sandia National Laboratories is a multimission laboratory managed and operated by National Technology and Engineering Solutions of Sandia, LLC., a wholly owned subsidiary of Honeywell International, Inc., for the U.S. Department of Energys National Nuclear Security Administration under contract DE-NA-0003525.

- 
- [1] For example, see Ref. [2] and other reviews such as C. Connaughton, S. Nazarenko, and B. Quinn, *Phys. Rep.* **604**, 1 (2015) and A. Fujisawa, *Nucl. Fusion* **49**, 013001 (2009).
  - [2] P. H. Diamond, S.-I. Itoh, K. Itoh, and T. S. Hahm, *Plasma Phys. Control. Fusion* **47**, R35 (2005).
  - [3] A. I. Smolyakov and P. H. Diamond, *Phys. Plasmas* **6**, 4410 (1999).
  - [4] A. I. Smolyakov, P. H. Diamond, and V. I. Shevchenko, *Phys. Plasmas* **7**, 1349 (2000).
  - [5] A. I. Smolyakov, P. H. Diamond, and M. Malkov, *Phys. Rev. Lett.* **84**, 491 (2000).
  - [6] M. A. Malkov, P. H. Diamond, and A. Smolyakov, *Phys. Plasmas* **8**, 1553 (2001).
  - [7] E.-J. Kim and P. H. Diamond, *Phys. Plasmas* **9**, 4530 (2002).
  - [8] P. Kaw, R. Singh, and P. H. Diamond, *Plasma Phys. Control. Fusion* **44**, 51 (2002).
  - [9] R. Trines, R. Bingham, L. O. Silva, J. T. Mendonça, P. K. Shukla, and W. B. Mori, *Phys. Rev. Lett.* **94**, 165002 (2005).
  - [10] K. Miki, P. H. Diamond, Ö. D. Gürçan, G. R. Tynan, T. Estrada, L. Schmitz, and G. S. Xu, *Phys. Plasmas* **19**, 092306 (2012).
  - [11] R. Singh, R. Singh, P. Kaw, Ö. D. Gürçan, and P. H. Diamond, *Phys. Plasmas* **21**, 102306 (2014).
  - [12] A. Fujisawa, K. Itoh, H. Iguchi, K. Matsuoka, S. Okamura, A. Shimizu, T. Minami, Y. Yoshimura, K. Nagaoka, C. Takahashi, M. Kojima, H. Nakano, S. Ohsima, S. Nishimura, M. Isobe, C. Suzuki, T. Akiyama, K. Ida, K. Toi, S.-I. Itoh, and P. H. Diamond, *Phys. Rev. Lett.* **93**, 165002 (2004).
  - [13] D. K. Gupta, R. J. Fonck, G. R. McKee, D. J. Schlossberg, and M. W. Shafer, *Phys. Rev. Lett.* **97**, 125002 (2006).
  - [14] J. C. Hillesheim, E. Delabie, H. Meyer, C. F. Maggi, L. Meneses, E. Poli, and JET Contributors, *Phys. Rev. Lett.* **116**, 065002 (2016).
  - [15] D. A. St-Onge, *J. Plasma Phys.* **83**, 905830504 (2017).
  - [16] J. B. Parker, *J. Plasma Phys.* **82**, 595820602 (2016).
  - [17] D. E. Ruiz, J. B. Parker, E. L. Shi, and I. Y. Dodin, *Phys. Plasmas* **23**, 122304 (2016).
  - [18] J. B. Parker and J. A. Krommes, *Phys. Plasmas* **20**, 100703 (2013).
  - [19] J. B. Parker and J. A. Krommes, *New J. Phys.* **16**, 035006 (2014).
  - [20] K. Srinivasan and W. R. Young, *J. Atmos. Sci.* **69**, 1633 (2012).
  - [21] N. C. Constantinou, B. F. Farrell, and P. J. Ioannou, *J. Atmos. Sci.* **73**, 2229 (2016).

- [22] J. E. Moyal, Proc. Cambridge Philosoph. Soc. **45**, 99 (1949).
- [23] E. Wigner, Phys. Rev. **40**, 749 (1932).
- [24] The iWKE was originally derived using CE2 in Ref. [16], where it was termed CE2-GO, and rederived using the WM formalism in Ref. [17], where it was termed WKE.
- [25] R. Numata, R. Ball, and R. L. Dewar, Phys. Plasmas **14**, 102312 (2007).
- [26] R. Singh, H. Jhang, and H. K. Kaang, Phys. Plasmas **23**, 074505 (2016).
- [27] B. N. Rogers, W. Dorland, and M. Kotschenreuther, Phys. Rev. Lett. **85**, 5336 (2000).
- [28] B. N. Rogers and W. Dorland, Phys. Plasmas **12**, 062511 (2005).
- [29] H.-L. Kuo, J. Meteor. **6**, 105 (1949).
- [30] J. A. Krommes and C.-B. Kim, Phys. Rev. E **62**, 8508 (2000).
- [31] G. W. Hammett, M. A. Beer, W. Dorland, S. C. Cowley, and S. A. Smith, Plasma Phys. Control. Fusion **35**, 973 (1993).
- [32] E. L. Shi, G. W. Hammett, T. Stoltzfus-Dueck, and A. Hakim, J. Plasma Phys. **83**, 905830304 (2017).
- [33] Details will be published in a separate paper.
- [34] For the lack of a better term, we call these driftons “runaway” by analogy with commonly known runaway electrons. However, the nature of the runaway effect for driftons is different as they are collisionless to begin with.
- [35] The supplementary materials are available at [www.princeton.edu/~idodin/wmsimulations/](http://www.princeton.edu/~idodin/wmsimulations/) (to be replaced with a permanent link).
- [36] Two calculations of  $\gamma_{\text{TI}}$  were proposed in Ref. [7] but are incomplete. The first one, which uses a Floquet analysis, misses the stability threshold determined by  $\varrho$ . (The  $q$ -dependent threshold that we discuss in the main text is absent in Ref. [7] because a different model of the electron response is assumed.) The second one, which uses the tWKE, is, in fact, a calculation of one of the ZI branches rather than of the TI. As we pointed out already, the tWKE cannot capture the TI in principle. In contrast,  $\gamma_{\text{TI}}$  reported in Ref. [15] is consistent with our Eq. (11).